

# From Sommerfeld and Brillouin forerunners to optical precursors

Bruno Macke and Bernard Ségard\*

*Laboratoire de Physique des Lasers, Atomes et Molécules ,  
CNRS et Université Lille 1, 59655 Villeneuve d'Ascq, France*

(Dated: October 4, 2018)

The Sommerfeld and Brillouin forerunners generated in a single-resonance absorbing medium by an incident step-modulated pulse are theoretically considered in the double limit where the susceptibility of the medium is weak and the resonance is narrow. Combining direct Laplace-Fourier integration and calculations by the saddle-point method, we establish an explicit analytical expression of the transmitted field valid at any time, even when the two forerunners significantly overlap. We examine how their complete overlapping, occurring for shorter propagation distances, originates the formation of the unique transient currently named resonant precursor or dynamical beat. We obtain an expression of this transient identical to that usually derived within the slowly varying envelope in spite of the initial discontinuity of the incident field envelope. The dynamical beats and  $0\pi$  pulses generated by ultra-short incident pulses are also briefly examined.

PACS numbers: 42.25.Bs, 42.50.Md, 41.20.Jb

## I. INTRODUCTION

About one century ago, in order to remove an apparent inconsistency between classical theory of waves and special relativity, Sommerfeld and Brillouin studied in detail the linear propagation of step-modulated light pulses in an absorbing medium with a single absorption line [1, 2]. They found that, at propagation distances such that the medium is opaque in a broad spectral range, the transmitted field consists of two successive transients preceding the establishment of the steady-state field at the carrier frequency  $\omega_c$  of the pulse (the “main field”). They naturally named the transients “forerunners”. *To be definite, we will conserve this name in the following, reserving the name of precursor to the unique transient occurring when the two forerunners completely overlap.* Sommerfeld and Brillouin showed that the first forerunner (the “Sommerfeld forerunner”) and the second one (the “Brillouin forerunner”) respectively involve frequencies large and small compared to the frequency  $\omega_0$  of the absorption line (that is in the spectral regions where the medium has some transparency). They proved that the front of the first one propagates at the velocity  $c$  of light in vacuum, in agreement with special relativity, and pointed out that the second one approximately moves at the group velocity at zero frequency. The shape of the forerunners was derived by means of classical complex analysis [1] and the newly developed saddle point method [2]. Later Brillouin used the stationary phase method to study his eponym forerunner when its formation is dominated by dispersion effects [3]. Following these pioneering works [4], the forerunners became a canonical problem in physics and entered reference textbooks in electromagnetism [5, 6]. More rigorous solutions, correcting the results obtained by Sommerfeld and Brillouin, were derived

by means of uniform asymptotic methods. See, e.g., [7–14]. The problem was also studied by a purely temporal approach instead of the usual spectral approach [15]. An abundant bibliography on forerunners can be found in [16]. For most recent studies related to the forerunners in the sense of Sommerfeld and Brillouin, see [17–20].

The expressions of the forerunners obtained in the most general case [9, 10] are tremendously complicated and not explicit. A good insight on the physics of forerunners is fortunately obtained by examining particular cases. We recently established simple analytical forms for the Sommerfeld and Brillouin forerunners when the propagation distance is such that the two forerunners are far away from each other [20]. In the present paper we study the problem when the electric susceptibility of the medium is weak and the resonance is narrow. This double condition is generally satisfied for dilute media in the entire optical domain but also for dense media in the  $X$  and  $\gamma$  spectral regions. We show that it is then possible to obtain explicit analytical expressions for the forerunners, valid even when the two forerunners significantly overlap, and to study how their complete overlapping originates the precursors actually observed in optics [21–27] or the dynamical beats evidenced in the experiments of nuclear coherent forward scattering [28, 29]. The arrangement of our paper is as follows. In Sec. II, we give the transfer function of the medium in the considered limit of weak susceptibility and narrow resonance. We establish in Sec. III the expressions of the Sommerfeld and Brillouin forerunners. We study in Sec. IV the evolution of the forerunners towards a unique transient (optical precursor or dynamical beat) and show that the expression of the latter is identical to that obtained within the slowly varying envelope approximation even when the envelope of the incident field is initially discontinuous. Finally the dynamical beats and  $0\pi$  pulses generated by ultra-short incident pulses are briefly revisited. We conclude in Sec. V by summarizing our main results.

\*Electronic address: bernard.segard@univ-lille-1.fr

## II. TRANSFER FUNCTION OF THE MEDIUM

We consider a one-dimensional electromagnetic wave propagating in the  $z$ -direction through an isotropic and homogeneous medium. Its electric field is assumed to be polarized in the  $x$ -direction ( $x, y, z$  : Cartesian coordinates). We denote  $e(0, t)$  the field at time  $t$  for  $z = 0$  (inside the medium) and  $e(z, t)$  its value after a propagation distance  $z$  through the medium. In a spectral approach the medium is characterized by its transfer function  $H(z, \omega)$  relating the Fourier transform  $E(z, \omega)$  of  $e(z, t)$  to that  $E(0, \omega)$  of  $e(0, t)$  [30].

$$E(z, \omega) = H(z, \omega)E(0, \omega). \quad (1)$$

The transmitted field, inverse Fourier transform of  $E(z, \omega)$ , reads as:

$$e(z, t) = \int_{-\infty}^{\infty} H(z, \omega)E(0, \omega)e^{i\omega t} \frac{d\omega}{2\pi}. \quad (2)$$

In all the following, we take for  $t$  a retarded time equal to the real time minus the luminal propagation time  $z/c$  (retarded-time picture). We have then

$$H(z, \omega) = \exp \left\{ -i\frac{\omega z}{c} \left[ \sqrt{1 + \chi(\omega)} - 1 \right] \right\}. \quad (3)$$

Here  $\chi(\omega)$  is the complex electric susceptibility of the medium at the frequency  $\omega$  and  $\sqrt{1 + \chi(\omega)}$  is its complex refractive index.  $\chi(\omega)$  being given, Eq.(2) can be numerically solved by fast Fourier transform (FFT) but has no exact analytical expression, even for the simplest forms of  $\chi(\omega)$ . Following Sommerfeld and Brillouin, most authors have considered a Lorentz medium consisting of an ensemble of damped harmonic oscillators with the same resonance frequency  $\omega_0$  and the same damping rate  $\gamma$ . Its susceptibility reads as:

$$\chi(\omega) = -\frac{\omega_p^2}{\omega^2 - \omega_0^2 - 2i\gamma\omega} \quad (4)$$

where  $\omega_p$  is the so-called plasma frequency whose square is proportional to the number density of absorbers. A very similar expression of the susceptibility is obtained for the two-level medium usually considered in quantum optics [31]. Without doing the usual rotating wave and slowly varying envelope approximations, we get:

$$\chi(\omega) = -\frac{\omega_p^2}{\omega^2 - \omega_0^2 - 2i\gamma\omega - \gamma^2} \quad (5)$$

with  $\omega_p^2 = 2\omega_0 p |\mu|^2 / \hbar \varepsilon_0$ . In this expression  $p$  is the difference of population per volume unit between the two levels at thermal equilibrium,  $\mu$  is the dipole moment matrix element of the transition and  $\gamma$  is the relaxation rate for the coherence. General properties of the transmitted field resulting from Eqs.(3-5) are discussed in [20]. It is

shown in particular that the very first beginning of the transmitted field always propagates without distortion at the velocity  $c$  and that its total area (to distinguish from that of its envelope) is conserved during the propagation.

The problem of the forerunners is greatly simplified in the double limit considered in the present paper where  $\gamma \ll \omega_0$  (narrow resonance) and  $|\chi(\omega)| \ll 1$  at every frequency (weak susceptibility). Due to the first condition the susceptibility of the two-level medium equals that of the Lorentz medium ( $\gamma^2$  negligible with regard to  $\omega_0^2$ ). The second condition is fulfilled when  $\omega_p^2 \ll 2\gamma\omega_0$ , that is, owing to the first condition, when  $\omega_p \ll \omega_0$ . The absorption coefficient for the amplitude  $\alpha(\omega)$  then takes the simple form  $\alpha(\omega) \approx -\frac{\omega}{2c} \text{Im}[\chi(\omega)]$ . It is everywhere small compared to the wavenumber  $k(\omega) = \omega/c$  and is maximum for  $\omega \approx \pm\omega_0$  with  $\alpha(\pm\omega_0) = \alpha_0 \approx \omega_p^2/(4\gamma c)$ . It is convenient to characterize the propagation distance by the corresponding optical thickness on resonance  $\alpha_0 z$ . The transfer function then reads as:

$$H(z, \omega) \approx \exp \left[ -\frac{i\omega z \chi(\omega)}{2c} \right] \approx \exp \left( \frac{2i\alpha_0 z \gamma \omega}{\omega^2 - \omega_0^2 - 2i\gamma\omega} \right). \quad (6)$$

Eq.(6) is obtained by expanding  $\sqrt{1 + \chi(\omega)}$  at the first order in  $\chi(\omega)$ . Its upper limit of validity is given by the condition :

$$\frac{\omega z}{c} \left| \sqrt{1 + \chi(\omega)} - \left[ 1 + \frac{\chi(\omega)}{2} \right] \right| \ll 1 \quad (7)$$

This condition has to be fulfilled at the frequencies  $\omega$  for which the medium has some transparency, say for which  $|H(\omega)| > 10^{-4}$ . For the parameters considered hereafter, numerical simulations show that Eq.(7) is over-satisfied for resonance optical thickness  $\alpha_0 z$  up to  $10^6$ .

An alternative form of  $H(z, \omega)$  can be obtained by expanding the exponent in Eq.(6) in partial fractions. It reads as  $H(z, \omega) = H_-(z, \omega) \cdot H_+(z, \omega)$  where

$$H_{\pm}(z, \omega) = \exp \left[ i\alpha_0 z \gamma \left( \frac{1 \pm i\gamma/\omega_0}{\omega \mp \omega_0 - i\gamma} \right) \right]. \quad (8)$$

Under this form, the transfer function is very similar to that encountered in the study of optical precursors in a medium with a transparency window between two absorption lines [32]. There is obviously some analogy between the two problems. It should be noticed, however, that the transfer function considered in [32] was associated with the envelope of the electric field whereas that given by Eq.(6) and Eq.(8) is associated with the field itself.

## III. SOMMERFELD AND BRILLOUIN FORERUNNERS

As Sommerfeld and Brillouin and most authors, we consider in this section a step-modulated incident field of the form  $e(0, t) = \sin(\omega_{ct}) \cdot u_H(t)$  where  $u_H(t)$  is the

Heaviside unit step function and  $\omega_c$  is the carrier frequency. Eq.(2) can then be reduced to

$$e(z, t) = \text{Im} \left[ \int_{\Gamma} \frac{H(z, \omega) e^{i\omega t}}{\omega - \omega_c} \frac{d\omega}{2i\pi} \right] \quad (9)$$

where  $\Gamma$  is a straight line parallel to the real axis passing under the pole at  $\omega = \omega_c$ . For the large propagation distances at which the forerunners are discernible, the medium is opaque in a broad spectral region and the ranges of action of  $H_+$  and  $H_-$  overlap. We assume here that  $\omega_c$  lies in the opacity region. The transmitted field  $e(z, t)$  then only contains high ( $\omega > \omega_c$ ) and low ( $\omega < \omega_c$ ) frequencies, respectively associated with the Sommerfeld and Brillouin forerunners. We write it :

$$e(z, t) = e_1(z, t) + e_2(z, t) \quad (10)$$

where  $e_1(z, t)$  and  $e_2(z, t)$  respectively stand for the first (Sommerfeld) forerunner and the second (Brillouin) forerunner. The forerunners are determined both by the frequency-dependence of the absorption of the medium and by its dispersion. The latter may be characterized by the group delay  $\tau_g(z, \omega) = -d\Phi/d\omega$  where  $\Phi(z, \omega)$  is the argument of  $H(z, \omega)$ . For the high and low frequencies associated with the Sommerfeld and Brillouin forerunners, respectively, we get the asymptotic forms

$$\tau_g(z, |\omega| \gg \omega_0) \approx \frac{2\alpha_0 z \gamma}{\omega_0^2} = t_B \frac{\omega_0^2}{\omega^2} \quad (11)$$

and

$$\tau_g(z, |\omega| \ll \omega_0) \approx t_B + \frac{6\alpha_0 z \gamma \omega^2}{\omega_0^4} = t_B \left( 1 + \frac{3\omega^2}{\omega_0^2} \right) \quad (12)$$

where

$$t_B = \frac{2\alpha_0 z \gamma}{\omega_0^2} = \tau_g(z, 0) - \tau_g(z, \infty) \quad (13)$$

$t_B$  is obviously indicative of the time-delay of the Brillouin forerunner with respect to the Sommerfeld forerunner and provides a good time scale for the study of both forerunners.

Eq.(11) and Eq.(12) show that the Sommerfeld forerunner will start at the *retarded time*  $t = 0$  with a infinitely large instantaneous frequency whereas the latter is vanishing for the Brillouin forerunner at  $t \approx t_B$ . As already numerically evidenced (see Fig.9 in [20]), the beginning of the forerunners will thus be well reproduced by using asymptotic forms for  $H(z, \omega)$  and  $E(0, \omega)$ . The transmitted field can then be calculated by direct integration of Eq.(9) by means of standard Laplace-Fourier procedures [20].

For the beginning of the Sommerfeld forerunner, we get [33]:

$$e_1(z, t) \approx \frac{\omega_c}{\omega_0} \sqrt{\frac{t}{t_B}} J_1(2\omega_0 \sqrt{t_B t}) e^{-2\gamma t} u_H(t) \quad (14)$$

where  $J_n(s)$  designates the Bessel function of the first kind of index  $n$ . For  $2\omega_0 \sqrt{t_B t} \gg 1$  the Bessel function may be replaced by its asymptotic form [34] to yield

$$e_1(z, t) \approx \frac{\omega_c}{\omega_0} \sqrt{\frac{2t}{\pi t_B}} \frac{\cos(2\omega_0 \sqrt{t_B t} - 3\pi/4)}{\sqrt{2\omega_0 \sqrt{t_B t}}} e^{-2\gamma t} u_H(t). \quad (15)$$

$J_1(s)$  equaling its asymptotic form for  $s \approx 2.47$ , the fields given by Eq.(15) and Eq.(14) are equal at the time  $t = t_1 \approx 1.52 / (\omega_0^2 t_B)$ .

Similarly we get for the beginning of the Brillouin forerunner [35]

$$e_2(z, t) \approx \frac{b}{\omega_c} \text{Ai}(-bt') e^{-2\gamma t'/3}. \quad (16)$$

Here  $b = [\omega_0^4 / (6\alpha_0 z \gamma)]^{1/3} = [\omega_0^2 / (3t_B)]^{1/3}$ ,  $t' = t - t_B$  and  $\text{Ai}(s)$  designates the Airy function. This solution is physically acceptable if and only if  $e_2(z, t) \approx 0$  for  $t \leq 0$ . This is achieved when  $\text{Ai}(bt_B) \approx 0$ , that is when  $\alpha_0 z \gg \omega_0 / \gamma$ . On the other hand, for  $bt' \gg 1$ , we get from the asymptotic form of  $\text{Ai}(-s)$  [34]

$$e_2(z, t) \approx \frac{\omega_0^{1/2}}{\pi^{1/2} \omega_c (3t_B t')^{1/4}} \sin \left( \frac{2\omega_0 t'^{3/2}}{3(3t_B)^{1/2}} + \frac{\pi}{4} \right) e^{-2\gamma t'/3}. \quad (17)$$

$\text{Ai}(-s)$  equaling its asymptotic form for  $s \approx 1.42$ , the fields given by Eq.(17) and Eq.(16) are equal at the *retarded time*  $t = t_2 \approx t_B + 1.42/b \approx t_B + 2.05 (t_B/\omega_0^2)^{1/3}$ .

The previous expressions of the forerunners are only valid up to a finite time, the longer the larger the propagation distance [20]. We find that the corrections to Eq.(14) [Eq.(16)] due to the next terms in the asymptotic expansion of  $\ln[H(z, \omega)]$  and of  $E(0, \omega)$  in powers of  $1/\omega$  [ $\omega$ ] are negligible up to  $t = t_1$  [ $t = t_2$ ] when the condition  $\alpha_0 z \gg \omega_0 / \gamma$  is satisfied. This condition thus suffices for the validity of Eq.(14) [Eq.(16)] for  $0 < t < t_1$  [ $0 < t < t_2$ ].

For  $t > t_1$  ( $t > t_2$ ), the Sommerfeld (Brillouin) forerunner is calculated by means of the basic saddle point method as used by Brillouin [2, 4]. Introducing the phase function  $\Psi(z, \omega) = i\omega t + \ln[H(z, \omega)]$ , Eq.(9) is rewritten as

$$e(z, t) = \text{Im} \left[ \int_{\Gamma} \frac{\exp[\Psi(z, \omega)]}{\omega - \omega_c} \frac{d\omega}{2i\pi} \right]. \quad (18)$$

The integral is calculated by deforming the straight line  $\Gamma$  in a contour travelling along lines of steepest descent of the function  $\Psi(z, \omega)$  from the saddle points where  $\partial\Psi/\partial\omega = 0$  [36]. The contribution of a nondegenerate saddle point at  $\omega_s$  to the integral reads as

$$a(\omega_s) = \frac{\exp[\Psi(\omega_s) + i\theta_s]}{i(\omega_s - \omega_c) \sqrt{2\pi\Psi''(\omega_s)}} \quad (19)$$

where  $\theta_s$  is the angle of the direction of steepest descent with the real axis and  $\Psi''(\omega_s)$  is a shortcut for  $\partial^2\Psi/\partial\omega^2$

at  $\omega = \omega_s$ . We may disregard the presence of the pole at  $\omega_c$ . The corresponding residue is indeed negligible when, as assumed here,  $\omega_c$  lies in the opacity region of the medium. The determination of the saddle points is very simple in the double limit considered in the present paper. Due to the weak susceptibility hypothesis, the equation giving the complex frequencies of the saddle points is only of fourth degree (instead of eighth degree in the general case) and the narrow-resonance condition allows us to solve this equation at the lowest order in  $\gamma$ . Regrouping the four solutions in two pairs, we easily get  $\omega_n^\pm = \pm\omega_n + i\gamma_n$  with  $n = 1, 2$  and

$$\omega_n = \omega_0 \sqrt{1 + \frac{t_B}{2t} \left[ 1 - (-1)^n \sqrt{1 + \frac{8t}{t_B}} \right]} \quad (20)$$

$$\gamma_n = \gamma \left[ 1 - \frac{(-1)^n}{\sqrt{1 + \frac{8t}{t_B}}} \right] \quad (21)$$

$$\theta(\omega_n^\pm) = \mp(-1)^n \frac{\pi}{4}. \quad (22)$$

The pair associated with  $\omega_1$  (high frequency) obviously originates the Sommerfeld forerunner and yields

$$e_1(z, t) = \text{Im} [a_1(\omega_1^+) + a_1(\omega_1^-)] \quad (23)$$

$$e_1(z, t) = \sqrt{\frac{2}{\pi}} \left( \frac{\omega_0 \omega_c}{\omega_1^2 - \omega_c^2} \right) \times \left( \frac{\cos [\omega_1 t + \omega_1 \omega_0^2 t_B / (\omega_1^2 - \omega_0^2) - 3\pi/4]}{\omega_0^2 \sqrt{t_B} \left[ (\omega_1 + \omega_0)^{-3} + (\omega_1 - \omega_0)^{-3} \right]} \right) e^{-\gamma_1' t} \quad (24)$$

where

$$\gamma_1' t = \gamma t + \frac{\gamma t_B}{4} \left( \sqrt{1 + \frac{8t}{t_B}} - 1 \right) \quad (25)$$

For  $t \ll t_B$ , Eq.(24) is reduced to Eq.(15), which itself fits Eq.(14) at the time  $t = t_1$ . This means that the fields given by Eq.(24) and Eq.(14) will fit together in  $t_1$  if  $t_1 \ll t_B$ . It is easily shown that this is achieved when  $\alpha_0 z \gg \omega_0/\gamma$ . The combination of Eq.(14) for  $t < t_1$  and Eq.(24) for  $t \geq t_1$  then provides an analytical expression of the Sommerfeld forerunner valid at every time.

A similar calculation for the pair of saddle points associated with  $\omega_2$  (low frequency) yields the Brillouin forerunner

$$e_2(z, t) = \sqrt{\frac{2}{\pi}} \left( \frac{\omega_0 \omega_c}{\omega_c^2 - \omega_2^2} \right) \times \left( \frac{\sin [\omega_2 t - \omega_2 \omega_0^2 t_B / (\omega_0^2 - \omega_2^2) + \pi/4]}{\omega_0^2 \sqrt{-t_B} \left[ (\omega_2 + \omega_0)^{-3} + (\omega_2 - \omega_0)^{-3} \right]} \right) e^{-\gamma_2' t'} \quad (26)$$

where

$$\gamma_2' t' = \gamma (t - t_B) - \frac{\gamma t_B}{4} \left( \sqrt{1 + \frac{8t}{t_B}} - 3 \right) \quad (27)$$

For  $t' = t - t_B \ll t_B$ , Eq.(26) is reduced to Eq.(17), which itself fits Eq.(16) at the time  $t_2$ . If  $t_2 - t_B \ll t_B$  (a condition also satisfied when  $\alpha_0 z \gg \omega_0/\gamma$ ), the Brillouin forerunner will thus be well reproduced by Eq.(16) for  $t < t_2$  and by Eq.(26) for  $t \geq t_2$ .

To summarize, when the propagation distance is such that  $\alpha(\omega_c)z \gg 1$  (opacity condition for the main field) and that  $\alpha_0 z \gg \omega_0/\gamma$ , the transmitted field is simply the sum of the Sommerfeld and Brillouin forerunners for which we have obtained piecewise analytical expressions valid in the entirety of the time domain where they have significant amplitude.

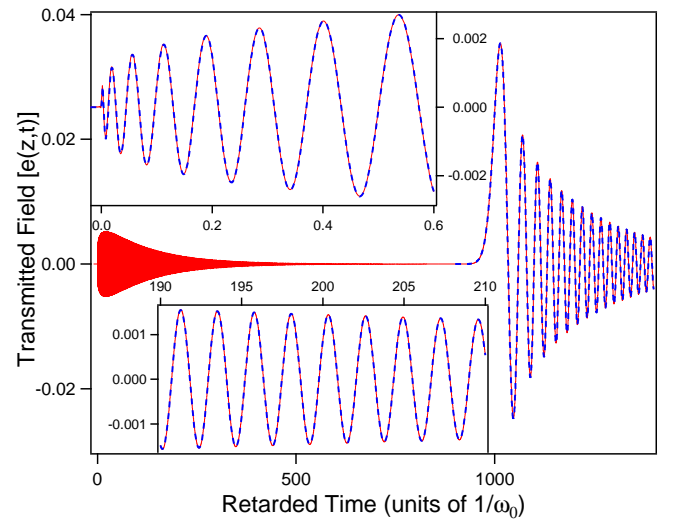


Figure 1: (Color online) Transmitted field  $e(z, t)$  for an incident field  $e(0, t) = \sin(\omega_c t) \cdot u_H(t)$ . Parameters  $\gamma = \omega_p = \omega_0/200$ ,  $\omega_c = \omega_0$  and  $\alpha_0 z = 10^5$ , for which  $\alpha_0 z \gamma / \omega_0 = 500$ ,  $\omega_0 t_B = 1000$  and  $\gamma t_B = 5$ . The full line (dashed line) is the exact numerical solution (our approximate analytical solution). For the considered parameters, the first (Sommerfeld) and second (Brillouin) forerunners are well separated. Upper (lower) inset: enlargement of the beginning (tail) of the Sommerfeld forerunner.

To illustrate our results, we consider first the case where the two forerunners are well separated. In order to meet the weak-susceptibility and narrow-resonance conditions, we take  $\gamma = \omega_p = \omega_0/200$ . Its damping time being of the order of  $1/\gamma$ , the Sommerfeld forerunner will not overlap the Brillouin forerunner if  $t_B \gg 1/\gamma$ , that is when  $\alpha_0 z \gg \omega_0^2 / (2\gamma^2)$ . Figure 1 shows the result obtained when  $\gamma t_B = 5$ , a value attained at a propagation distance  $z$  such that  $\alpha_0 z = 10^5$  for which  $\omega_0 t_B = 1000$ ,  $\omega_0 t_1 \approx 1.52 \times 10^{-3}$  and  $\omega_0 (t_2 - t_B) \approx 20.5$ . As expected, our piecewise analytical solution perfectly fits at every time the exact numerical solution obtained by using the transfer function given by Eq.(3) and Eq.(4) without any approximation. It is worth noticing that the maximum

of the Brillouin forerunner occurs at a time shorter than  $t_B$  and that  $\gamma(t_B - t_B) \ll 1$ . Eq.(16) then shows that the corresponding amplitude is proportional to  $b \propto z^{-1/3}$  and inversely proportional to  $\omega_c$ , *no matter the location of  $\omega_c$  in the opacity region, inside or outside the anomalous dispersion region*. We also remark that, for the large optical thickness considered in this example, the asymptotic form of the Sommerfeld forerunner given by Eq.(14) holds much beyond  $t_1$ . This equation even provides a good estimate of the maximum amplitude of the forerunner that occurs at  $t \approx 1/(8\gamma)$  and is proportional to  $\omega_c$ . We have checked all these points by comparing the exact numerical results obtained for  $\omega_c$  equal to  $\omega_0$  (Fig.1),  $\omega_0\sqrt{2}$  and  $\omega_0/\sqrt{2}$ .

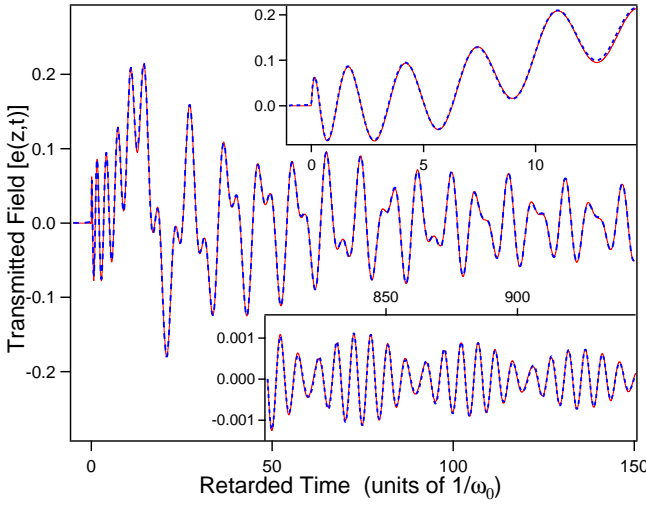


Figure 2: (Color online) Same as Fig. 1 for  $\alpha_0 z = 1000$  ( $\alpha_0 z \gamma / \omega_0 = 5$ ,  $\omega_0 t_B = 10$ , and  $\gamma t_B = 1/20$ ). The two forerunners significantly overlap but remain discernible. The upper inset clearly shows the oscillations of the Sommerfeld forerunner superimposed over the slow rise of the Brillouin forerunner. In the far wing (lower inset) appear clean beatings that anticipate what will become the optical precursor.

In the previous example, the condition of validity of our analytical results ( $\alpha_0 z \gg \omega_0 / \gamma$ ) was over-satisfied. Figure 2 shows, other things being equal, the result obtained for a propagation distance 100 times shorter, for which  $\alpha_0 z \gamma / \omega_0 = 5$ ,  $\omega_0 t_B = 10$ ,  $\omega_0 t_1 \approx 0.15$  and  $\omega_0(t_2 - t_B) \approx 4.4$ . Though the condition of validity of our approximations is then marginally satisfied, our piecewise analytical solution continues to fit very well the exact numerical solution. Since  $t_B$  is now much shorter than  $1/\gamma$  ( $\gamma t_B = 1/20$ ), the Sommerfeld forerunner significantly overlaps that of Brillouin. It remains quite visible for  $t < t_B$  where it is superimposed to the slow rise of the latter (see upper inset of Fig.2). For  $t > t_B$ , beatings between the two forerunners are observed [17]. They are well developed when the instantaneous frequencies  $\omega_1$  and  $\omega_2$  of the forerunners are close and their amplitudes are comparable. This occurs when  $\sqrt{t/t_B} \gg 1$  [see Eqs.(20, 24, 26)]. In the present case, the corresponding

times are long compared to the damping time  $1/\gamma$  and the amplitude of the beats is weak (see lower inset of Fig.2).

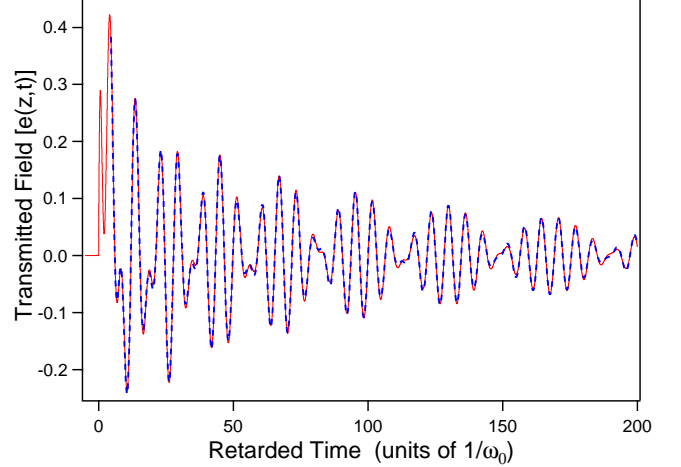


Figure 3: (Color online) Same as Fig. 1 for  $\alpha_0 z = 200$  ( $\alpha_0 z \gamma / \omega_0 = 1$  and  $\omega_0 t_B = 2$ ). A sole oscillation of the Sommerfeld forerunner is visible and clean beats appear sooner with significant amplitude. The analytical solution (dashed line) is only given in the time domain  $t \geq t_2$  where it is reduced to the saddle point solution (see text).

For smaller propagation distances (that is for shorter times  $t_B$ ), clean beatings are expected to appear sooner with larger amplitudes. This is illustrated Fig.3 obtained for  $\alpha_0 z \gamma / \omega_0 = 1$ , that is for  $\alpha_0 z = 200$  with our parameters. We have then  $\omega_0 t_B = 2$ ,  $\omega_0 t_1 \approx 0.76$  and  $\omega_0 t_2 \approx 4.58$ . For  $t \leq t_2$ , a single oscillation of the Sommerfeld forerunner is still visible. Since the condition  $\alpha_0 z \gamma / \omega_0 \gg 1$  is not satisfied, it should be noticed that our piecewise solutions for  $e_1(z, t)$  and  $e_2(z, t)$  fail in this time domain. On the other hand, the latter continue to perfectly fit the exact numerical solutions for  $t > t_2$ , a domain where they are reduced to the solutions given by the saddle point method [Eqs.(24, 26)]. As we shall see later, these solutions remain a good approximation for  $t > t_2$  as long as the medium is opaque at the carrier frequency.

Finally when the propagation distance still decreases to become such that  $\alpha_0 z \gamma / \omega_0 \ll 1$  and thus  $\omega_0 t_B \ll 1$ , the two forerunners completely overlap to originate the unique transient currently called resonant precursor [17, 37], Sommerfeld-Brillouin precursor [23] or dynamical beat [29]. It is then possible to obtain an analytical expression of the transmitted field valid at every time, no matter the optical thickness  $\alpha_0 z$ .

#### IV. OPTICAL PRECURSORS OR DYNAMICAL BEATS

This study is facilitated by writing the field under the form  $e(z, t) = \text{Re} [e_0(z, t) e^{i\omega_0 t}]$  where  $e_0(z, t)$  is the com-

plex envelope of the field in a frame rotating at the angular velocity  $+\omega_0$ . We consider an incident field  $e(0, t) = \text{Re} [f(t) e^{i\omega_c t}]$  that generalizes that considered in Sec.III. Its complex envelope reads as  $e_0(0, t) = f(t) e^{i\Delta t}$  where  $\Delta = \omega_c - \omega_0$  is assumed to be small compared to  $\omega_0$ . Eq.(2) then leads to

$$e_0(z, t) = e^{-i\omega_0 t} \int_{\Gamma} H(z, \omega) F(\omega - \omega_c) e^{i\omega t} \frac{d\omega}{2\pi} \quad (28)$$

where  $F(\omega)$  is the Fourier transform of  $f(t)$ . When  $\alpha_0 z \gamma / \omega_0 \ll 1$  as considered in all this section, the partial transfer functions  $H_+(z, \omega)$  and  $H_-(z, \omega)$  defined Eq.(8) significantly differ from 1 only in narrow domains around  $+\omega_0$  and  $-\omega_0$ , respectively. It is then justified to make the so-called rotating wave approximation [31] and to approximate  $H(z, \omega)$  in Eq.(28) by  $H_+(z, \omega)$ . Translating the frequencies by  $-\omega_0$  in the integral, we get

$$e_0(z, t) = \int_{\Gamma} H_0(z, \omega) F(\omega - \Delta) e^{i\omega t} \frac{d\omega}{2\pi} \quad (29)$$

where

$$H_0(z, \omega) = \exp \left[ -\alpha_0 z \gamma \left( \frac{1 + i\gamma/\omega_0}{\gamma + i\omega} \right) \right] \approx \exp \left( -\frac{\alpha_0 z \gamma}{\gamma + i\omega} \right) \quad (30)$$

Here  $H_0(z, \omega)$  is nothing else than the *transfer function for the field envelope* and characterizes the medium *independently of the incident field*. The corresponding impulse response is easily obtained by inverse Laplace transform and reads as

$$h_0(z, t) = \delta(t) - \sqrt{\frac{\alpha_0 z \gamma}{t}} J_1(2\sqrt{\alpha_0 z \gamma t}) e^{-\gamma t} u_H(t) \quad (31)$$

where  $\delta(t)$  is the Dirac delta function. On the other hand  $F(\omega - \Delta)$  is the Laplace-Fourier transform of  $f(t) e^{i\Delta t}$  and we get from Eq. (29):

$$e_0(z, t) = h_0(z, t) \otimes [f(t) e^{i\Delta t}] \quad (32)$$

Combined with the relation  $e(z, t) = \text{Re} [e_0(z, t) e^{i\omega_0 t}]$ , Eq.(32) enable us to determine the transmitted field for arbitrary modulation of the envelope of the incident field. When the latter is step modulated, that is when  $f(t) \propto u_H(t)$ , the convolution of Eq.(32) is easily calculated. Replacing this result in the expression of  $e(z, t)$ , we finally obtain the transmitted fields for the incident fields  $\sin(\omega_c t) u_H(t)$  and  $\cos(\omega_c t) u_H(t)$ . They respectively read as  $\text{Im} [\tilde{e}(z, t)]$  and  $\text{Re} [\tilde{e}(z, t)]$  with

$$\tilde{e}(z, t) = \left[ 1 - \int_0^t \sqrt{\frac{\alpha_0 z \gamma}{\theta}} J_1(2\sqrt{\alpha_0 z \gamma \theta}) e^{-(\gamma+i\Delta)\theta} d\theta \right] \times e^{i\omega_c t} u_H(t) \quad (33)$$

In agreement with the Feynmann analysis of the absorption and dispersion phenomena in linear media [38], Eq.(33) makes explicit in both cases that the transmitted wave is the sum of the incident wave as it would propagate in vacuum and of the secondary wave radiated by the polarization induced in the medium, initially of zero amplitude [22, 39]. Results equivalent or analog to those given Eqs.(31-33) were established in the past [28, 37, 39-41, 43-47]. However they were generally obtained in the frame of the slowly varying envelope approximation (SVEA) [31]. As soundly remarked in [48], its use is quite disputable when the envelope is initially discontinuous. SVEA is not made in our calculations. In order to check the validity of the latter, we compare Fig.4 the fields derived from Eq.(33) to the exact numerical solution for  $\alpha_0 z = 20$ , with  $\gamma$  and  $\omega_p$  as in Sec.III. We

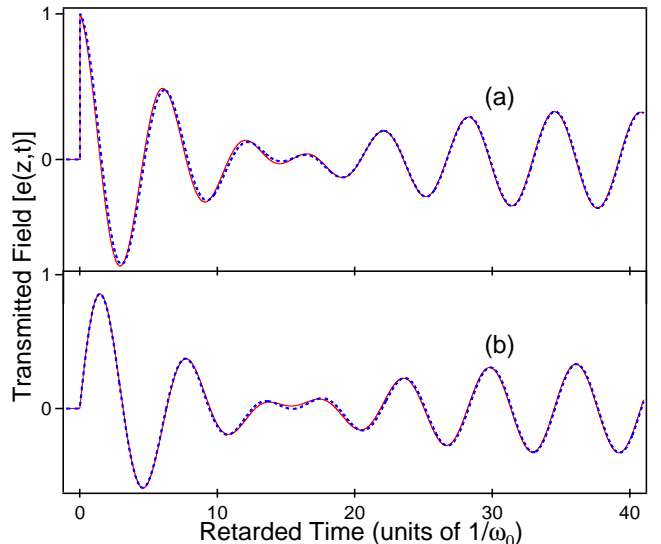


Figure 4: (Color online) Transmitted field (optical precursor) obtained with incident fields (a)  $\cos(\omega_c t) \cdot u_H(t)$  and (b)  $\sin(\omega_c t) \cdot u_H(t)$  for  $\alpha_0 z = 20$  ( $\alpha_0 z \gamma / \omega_0 = 1/10$ ). In both cases, the analytical solution obtained within the rotating wave approximation (dashed line) very satisfactorily fits the exact numerical solution (full line).

have then  $\alpha_0 z \gamma / \omega_0 = 1/10$ . The agreement between the two solutions is very satisfactory, even when the incident field itself is discontinuous (curve a). The discrepancy is everywhere smaller than  $\alpha_0 z \gamma / \omega_0$ , which is the order of magnitude of the deviation of  $H_{\pm}(z, \mp\omega_0)$  from unity.

Although precursors are not generated in this case, we incidentally mention that Eq.(33) admits an explicit solution when the incident field is significantly detuned from resonance ( $\Delta \gg \gamma, \alpha_0 z$ ). The exponential  $e^{i\Delta t}$  is then rapidly variable compared to the rest of the integrand and a simple integration per part yields

$$e(z, t) \approx \sin(\omega_c t) + \frac{\alpha_0 z \gamma}{\Delta} \left[ \cos(\omega_c t) - \frac{J_1(2\sqrt{\alpha_0 z \gamma t})}{\sqrt{\alpha_0 z \gamma t}} e^{-\gamma t} \cos(\omega_0 t) \right] \quad (34)$$

where the multiplication by  $u_H(t)$  has been omitted for simplicity. The first term in Eq.(34) is the incident field which is transmitted with negligible attenuation when  $\Delta \gg \gamma\alpha_0 z$  whereas the second term evidences a beat between the incident field and the field reemitted by the medium at its eigenfrequency. Since  $J_1(s) \rightarrow s/2$  for  $s \rightarrow 0$ , the initial amplitude of the beat is zero, as expected. A convincing experimental demonstration of such beats can be found in [49]. When  $\alpha_0 z \ll 1$ , the beat is reduced to  $\frac{\alpha_0 z \gamma}{\Delta} [\cos(\omega_{ct}) - e^{-\gamma t} \cos(\omega_0 t)]$ . This condition is approximately met in the experiments reported in [50].

Precursors are obtained in the opposite case where the incident field is resonant or quasi resonant ( $\Delta \ll \gamma, \gamma\alpha_0 z$ ). *We restrict the analysis to this case in the following.* The envelope  $e_0(z, t)$  of the transmitted field is then real and can be written as

$$e_0(z, t) \approx \left( 1 - \alpha_0 z \int_0^t \frac{J_1(2\sqrt{\alpha_0 z \theta})}{\sqrt{\alpha_0 z \theta}} e^{-\theta} d\theta \right) u_H(t). \quad (35)$$

It takes a simplified form when the Bessel function in the integral evolves rapidly with respect to the exponential, that is when  $\alpha_0 z \gg 1, \Delta/\gamma$ . Again by an integration per parts, Eq.(35) then yields  $e_0(z, t) \approx J_0(2\sqrt{\alpha_0 z \gamma t}) e^{-\gamma t} u_H(t)$  and the transmitted field for  $e(0, t) = \sin(\omega_{ct}) u_H(t)$  reads as:

$$e(z, t) \approx J_0(2\sqrt{\alpha_0 z \gamma t}) \sin(\omega_0 t) e^{-\gamma t} u_H(t). \quad (36)$$

It consists of successive lobes of decreasing amplitude and increasing duration, separated by zeroes of amplitude occurring at times  $t = j_{0p}^2/(4\alpha_0 z \gamma)$ , where  $j_{0p}$  is the zero of order  $p$  of  $J_n(s)$ . Fig. 5 (curve a) shows that this approximate analytical solution satisfactorily fits the exact numerical solution. As announced in Sec.III and shown Fig.5 (curve b), this is also true for  $t > t_2$  for the saddle point solution. This simply results from the fact that  $t_2 \gg t_B$  with  $\omega_0 t_B \ll 1$  and that the two solutions have then the same asymptotic form for  $t \gg t_B$ .

When  $\alpha_0 z$  decreases, our saddle point approximation becomes worst and worst owing to the coalescence of  $\omega_1$ ,  $\omega_2$  and  $\omega_0$  in a time domain where  $\exp(-\gamma t) = O(1)$  whereas the rotating wave approximation becomes better and better. Correlatively the number of lobes in  $e(z, t)$  and of zeroes for the amplitude decreases. Of special interest is the case where there is a single zero of amplitude. The integral in Eq.(35) having its first maximum (absolute maximum) for  $2\sqrt{\alpha_0 z \gamma t} = j_{11}$ , this will obviously occur when this maximum is equal to 1, that is when

$$\int_0^{j_{11}^2/4} \frac{J_1(2\sqrt{\theta})}{\sqrt{\theta}} \exp\left(-\frac{\theta}{\alpha_0 z}\right) d\theta = 1. \quad (37)$$

This equation in  $\alpha_0 z$  is easily solved by numerical procedures to yield  $\alpha_0 z \approx 2.80$ , the zero of amplitude being attained at the time  $t = t_c$  such that  $\gamma t_c = j_{11}^2/(4\alpha_0 z)$ .

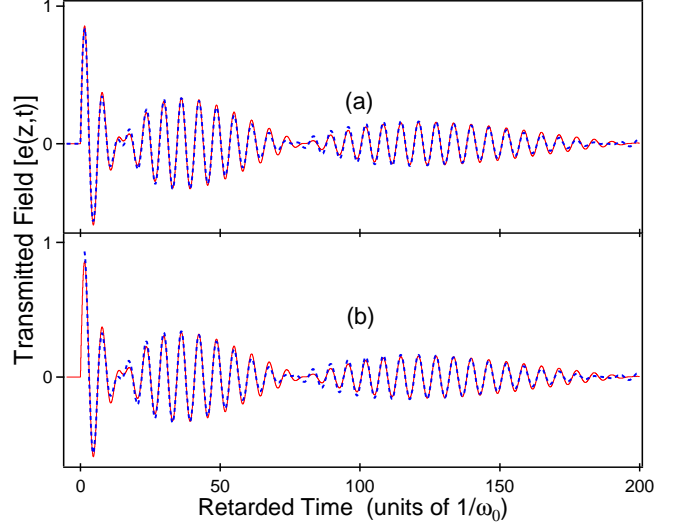


Figure 5: (Color online) Extended view of the precursor obtained in the conditions of Fig.4 with  $e(0, t) = \sin(\omega_{ct}) \cdot u_H(t)$ . The exact numerical solution (full line) is compared (a) to the simple solution given by Eq.(36) and (b) to the saddle point solution for  $t \geq t_2$  (dotted line).

This solution is general and does not depend on a particular choice of parameters. Figure 6 shows the transmitted

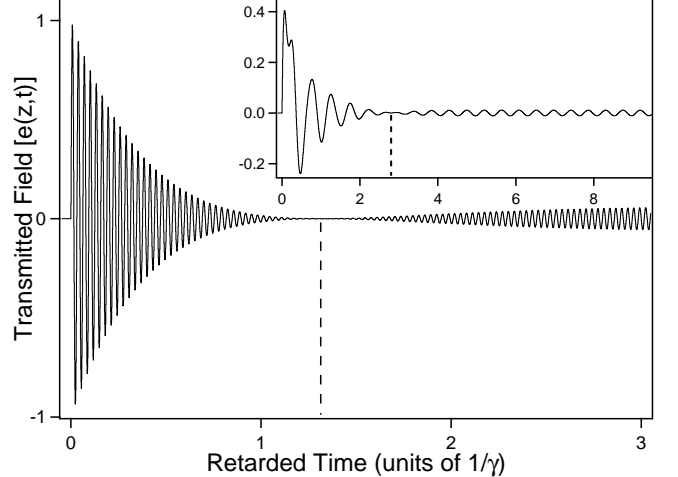


Figure 6: Transmitted field as a function of  $\gamma t$  for  $\alpha_0 z = 2.80$ . The precursor has a sole lobe and its amplitude falls to 0 for  $\gamma t = \gamma t_c \approx 1.31$  (vertical dashed line). The field amplitude then progressively rises to its steady state value  $\exp(-2.80) \approx 0.061$ . The inset shows the similar behavior numerically obtained for  $\alpha_0 z \approx 4.5$  with the Brillouin parameters, namely  $\gamma/\omega_0 = 0.071$  and  $\omega_p/\omega_0 = 1.11$ .

field obtained for  $\alpha_0 z = 2.80$  with our parameters. The field amplitude actually cancels for  $\gamma t \approx 1.31$  and, as expected, the precursor consists of an unique lobe that clearly precedes the arrival of the main field of steady state amplitude  $e^{-2.8} \approx 0.061$ . The values  $\alpha_0 z \approx 2.80$  and  $\gamma t_c \approx 1.31$  are obviously specific to the weak sus-

ceptibility and narrow resonance limit considered in the present paper but a numerical exploration shows that comparable values are obtained with the parameters considered by Brillouin (see pp.55-57 in [4]). A precursor with a single lobe is then obtained for  $\alpha_0 z \approx 4.5$  with  $\gamma t_c \approx 2.80$  (see inset in Fig.6).

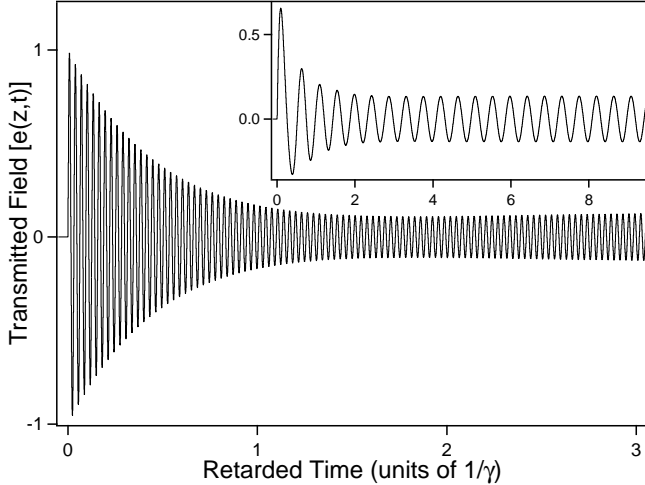


Figure 7: Transmitted field as a function of  $\gamma t$  for  $\alpha_0 z = 2$ . Inset: corresponding numerical result with the Brillouin parameters.

For shorter propagation distances, the precursor, if it exists, is less and less distinguishable from the main field that becomes larger and larger. Figure 7 shows the analytical result derived from Eq.(35) for  $\alpha_0 z = 2$ . There is only a hardly visible minimum of amplitude between the precursor and the main field. The numerical solution obtained for the same optical thickness with the Brillouin parameters shows a similar behavior (see inset in Fig.7). When  $\alpha_0 z \ll 1$  (optically thin medium limit), the envelope of the transmitted pulse takes the asymptotic form

$$e_0(z, t) \approx [1 - \alpha_0 z (1 - e^{-\gamma t})] u_H(t). \quad (38)$$

One only observes in this case an exponential fall of the field amplitude from 1 to its steady state value  $\exp(-\alpha_0 z) \approx 1 - \alpha_0 z$ . Eq.(38) gives a not too bad approximation of the exact result for an optical thickness of 0.5 (1 for the intensity) as considered in [25].

It is assumed in the previous calculations that the initial rise of the envelope of the incident field is instantaneous. In real experiments, the rise time  $T_r$  is obviously finite and rise time effects may prevent the excitation of the Sommerfeld and Brillouin forerunners [19, 20]. The situation is better for the precursors [22, 25, 26]. An examination of Eq.(31) and Eq.(32) in the resonant case indeed shows that the rise-time effects will be negligible if  $\gamma T_r \ll 1$  and  $\alpha_0 z \gamma T_r \ll 1$ . Only the first condition is usually considered in the literature. It is clearly not sufficient for the large optical thickness required to obtain well-developed precursors. In the millimeter-wave experiment on a molecular absorber reported in [22],  $\alpha_0 z \approx 70$

and  $\gamma T_r \approx 3 \times 10^{-3}$ . We have then  $\alpha_0 z \gamma T_r \approx 0.2$  and the intensity profile  $J_0^2(2\sqrt{\alpha_0 z \gamma t}) e^{-2\gamma t} u_H(t)$  predicted by Eq.(36) is well reproduced, except for the initial intensity slightly smaller than 1. On the other hand the optical experiments on a cloud of cold atoms reported in [26] show that the amplitude (the shape) of the precursor may be considerably reduced (modified) when the condition  $\alpha_0 z \gamma T_r \ll 1$  is not satisfied even when the condition  $\gamma T_r \ll 1$  holds. Fig.4 in [26] gives an example where the peak intensity of the precursor is reduced by about one order of magnitude with a second lobe larger than the first one.

In the spirit of the pioneering work by Sommerfeld and Brillouin, we have considered up to now step-modulated incident pulses. The case where the step  $u_H(t)$  is replaced by a single-sided exponential  $e^{-\Gamma t} u_H(t)$  is considered in [23, 28]. In the optical experiment reported in [23], such pulses are obtained by passing ultra-short laser pulses through a Fabry-Pérot resonator and the rate  $\Gamma$  is the damping rate of the resonator. In the nuclear forward scattering experiment reported in [28],  $\Gamma$  is the decay rate of the 14.4 keV-state of  $^{57}\text{Fe}$  used as source. In both cases  $\Gamma \ll \omega_0$  and the rotating wave approximation holds. The envelope  $e_0(z, t)$  of the transmitted field is easily determined by replacing  $u_H(t)$  by  $e^{-\Gamma t} u_H(t)$  in the calculations leading to Eq.(35). We get:

$$e_0(z, t) \approx \left( 1 - \alpha_0 z \int_0^t \frac{J_1(2\sqrt{\alpha_0 z \theta})}{\sqrt{\alpha_0 z \theta}} e^{-(1-\Gamma/\gamma)\theta} d\theta \right) \times e^{-\Gamma t} u_H(t) \quad (39)$$

A very simple result is obtained in the nuclear forward scattering experiment where the source and the absorber are made of the same material. We have then  $\Gamma = \gamma$  and the envelope takes the form  $e_0(z, t) \approx J_0(2\sqrt{\alpha_0 z \gamma t}) e^{-\gamma t} u_H(t)$ , exact whatever  $\alpha_0 z$  may be.

New experiments of resonant nuclear forward scattering in optically thick samples were achieved in the 1990's by using synchrotron radiation instead of radioactive sources. For a review, see for example [29]. The generated transients were named dynamical beats. Their theoretical study is very simple in the case of a single line. Indeed the duration  $\tau_p$  of the synchrotron pulses used in these experiments is long compared to  $1/\omega_0$  but extremely short compared to  $1/\gamma$  and very short compared to  $1/(\alpha_0 z \gamma)$  (typically  $10^3$  smaller). The rotating wave approximation is then justified and the convolution product of Eq.(32) is reduced to

$$e_0(z, t) \approx f(t) - \alpha_0 z \gamma A \frac{J_1(2\sqrt{\alpha_0 z \gamma t})}{\sqrt{\alpha_0 z \gamma t}} e^{-\gamma t} u_H(t). \quad (40)$$

Here  $A = \int_{-\infty}^{+\infty} f(t) dt$  is the area of the incident field envelope (to distinguish from that of the incident field itself considered in Sec.II). This result is consistent with that given by Eq.(2.4) in [29] and with the experimental observations (see Fig.2 and Fig.3 in this reference).

Experiments were also achieved in optics by using ultra-short laser pulses. See, e.g., [21, 24, 51]. In the experiments on a semiconductor crystal (exciton transition) [51] and for the largest optical thicknesses considered in the experiments on an atomic vapor [21, 24], the condition  $\tau_p \ll 1/(\alpha_0 z \gamma)$  is not satisfied. The envelope of the transmitted pulse (polariton beat or  $0\pi$  pulse) then differs from that given by Eq.(40) and can only be determined by numerical calculations of the convolution product  $h_0(z, t) \otimes f(t)$ . It should however be noticed that, even when  $\alpha_0 z \gamma \tau_p = O(1)$  as in the case considered Fig.3c in [24], the solution given by Eq.(40) fits fairly well the exact solution for retarded times exceeding a few  $\tau_p$ . This explains in particular why the successive minimums of the transient observed in [51] at large enough retarded times occur at the times predicted by Eq.(40). In agreement with Crisp [41], we emphasize that, in all cases, the observed transient cannot be identified to the Sommerfeld forerunner as imprudently stated in [52]. This erroneous claim originates from confusion of the *field* given by Eq.(14) in the limit  $\alpha_0 z \gamma / \omega_0 \rightarrow \infty$  (Sommerfeld forerunner) with the *envelope of the field* given by Eq.(31) and Eq.(32) when  $\alpha_0 z \gamma / \omega_0 \ll 1$ . See also [53].

## V. CONCLUSION

We have studied in detail what become the Sommerfeld and Brillouin forerunners generated by an incident step

modulated pulse in a single-resonance absorbing medium when the propagation distance decreases. Analytical calculations, combining direct Laplace-Fourier integration and basic saddle point method, have been made possible by considering the double limit where the resonance is narrow and the medium susceptibility is weak. We have shown that the structure of the transmitted field only depends on  $\omega_0/\gamma$  and  $\alpha_0 z$  ( $\omega_0$  resonance frequency,  $\gamma$  resonance width,  $\alpha_0 z$  resonance optical thickness). The Sommerfeld and Brillouin forerunners are well apart for propagation distances  $z$  such that  $\alpha_0 z \gg \omega_0^2/(2\gamma^2)$  (Fig.1), they overlap but remain discernible if  $\alpha_0 z \gg \omega_0/\gamma$  (Fig.2) and become practically indiscernible (Fig.3) when  $\alpha_0 z = O(\omega_0/\gamma)$ . Finally, they originate clean beats (Fig.4 and Fig.5) when  $1 \ll \alpha_0 z \ll \omega_0/\gamma$ . These beats are nothing else than the optical precursor or dynamical beat actually observed in various spectral domains. A remarkable feature is obtained for  $\alpha_0 z = 2.80$  irrespective of the value of  $\omega_0/\gamma$ . The precursor then consists in a unique lobe clearly preceding the establishment of the steady-state field (Fig.6). For shorter propagation distances, the precursor, if it exists, is less and less distinguishable from the steady-state field that becomes larger and larger (Fig.7). All our analytical results on optical precursors are obtained without making the slowly varying approximation and are general. They are applied to other modulation schemes that the step modulation, in particular to revisit the dynamical beats, polariton beats and  $0\pi$  pulses generated by ultra-short incident pulses.

---

[1] A. Sommerfeld, Ann. Phys. (Leipzig) **44**, 177 (1914).  
[2] L. Brillouin, Ann. Phys. (Leipzig) **44**, 203 (1914).  
[3] L. Brillouin, in *Comptes Rendus du Congrès International d'Electricité, Paris 1932* (Gauthier-Villars, Paris 1933), Vol.2, pp 739-788.  
[4] Adaptations in English of [1-3] can be found in the book by L. Brillouin, *Wave Propagation and Group Velocity* (Academic Press, New York 1960), See Chaps. II-V.  
[5] J.A. Stratton, *Electromagnetic Theory* (McGraw-Hill, New York 1941).  
[6] J. D. Jackson, *Classical Electrodynamics*, 2nd ed. (Wiley, New York 1975).  
[7] V.A. Vasilev, M.Y. Kelbert, I.A. Sazonov and I.A. Chaban, Opt. Spectrosc. **64**, 862 (1988) [Opt. Spectrosc. **64**, 513 (1988)].  
[8] K.E. Oughstun and G.C. Sherman, J. Opt. Soc. Am. B **5**, 817 (1988).  
[9] K.E. Oughstun and G.C. Sherman, J. Opt. Soc. Am. A **6**, 1394 (1989).  
[10] K. E. Oughstun and G. C. Sherman, Phys. Rev. A **41**, 6090 (1990).  
[11] A. Ciarkowski, J. Tech. Phys. (Warsaw, Pol.) **43**, 187 (2002).  
[12] A. Ciarkowski, J. Tech. Phys. (Warsaw, Pol.) **44**, 181 (2003).  
[13] N. A. Cartwright and K. E. Oughstun, SIAM Rev. **49**, 628 (2007).  
[14] A. Ciarkowski, Int. J. Electron. Telecommun. **57**, 251 (2011).  
[15] A. Karlsson and S. Rike, J. Opt. Soc. Am. A **15**, 487 (1998).  
[16] K.E. Oughstun, *Electromagnetic and Optical Pulse Propagation 2 : Temporal Pulse Dynamics in Dispersive Attenuative Media* (Springer, New York, 2009).  
[17] H. Jeong, U.L. Österberg, and T. Hansson, J. Opt. Soc. Am. B **26**, 2455 (2009).  
[18] K.E. Oughstun, N.A. Cartwright, D.J. Gauthier, and H. Jeong, J. Opt. Soc. Am. B **27**, 1664 (2010).  
[19] B. Macke and B. Ségar, J. Opt. Soc. Am. B **28**, 450 (2011).  
[20] B. Macke and B. Ségar, Phys. Rev. A **86**, 013837 (2012).  
[21] J.E. Rothenberg, D. Grischkowsky, and A.C. Balant, Phys. Rev. Lett. **53**, 552 (1984).  
[22] B. Ségar, J. Zemmouri, and B. Macke, Europhys. Lett. **4**, 47 (1987). See Fig.2 in this reference.  
[23] J. Aaviksoo, J. Kuhl, and K. Ploog, Phys. Rev. A **44**, 5353(R) (1991).  
[24] M. Matusovsky, B. Vaynberg, and M. Rosenbluh, J. Opt. Soc. Am. B **13**, 1994 (1996).  
[25] H. Jeong, A. M. C. Dawes, and D. J. Gauthier, Phys. Rev. Lett., **96**, 143901 (2006).  
[26] Dong Wei, J.F. Chen, M.M.T. Loy, G.K.L. Wong, and S. Du, Phys. Rev. Lett. **103**, 093602 (2009).  
[27] B. Macke and B. Ségar, Phys. Rev. A **81**, 015803 (2010). See Fig.1 in this paper.  
[28] F.J. Lynch, R.E. Holland, and M. Hammermesh, Phys.

Rev. **120**, 513 (1960).

[29] U. van Bürck, Hyp. Interact. **123/124**, 483 (1999).

[30] We use the definitions, sign conventions and results of the linear system theory. See for example A.Papoulis, *The Fourier Integral and its Applications* (Mc Graw Hill, New York 1987).

[31] L. Allen and J.H. Eberly, *Optical resonance and two-level atoms* (Dover, New York, 1987).

[32] B. Macke and B. Ségard, Phys. Rev. A **80**, 011803(R) (2009).

[33] See Eq.(21) in [20], with the correspondence  $\xi = \omega_p^2 z / 2c = 2\alpha_0 z \gamma = \omega_0^2 t_b$ .

[34] *Handbook of Mathematical functions*, edited by M. Abramowitz and I. A. Stegun (Dover, New York, 1972).

[35] See Eq.(36) in [20]. It is assumed in using this equation that  $\gamma \ll b$ . In the weak-susceptibility and narrow-resonance limit considered in the present paper, this condition is always satisfied except for huge propagation distances.

[36] J. Mathews and R.L. Walker, *Mathematical Methods of Physics* (Benjamin, New York 1965). Sec. 3-6.

[37] E. Varoquaux, G. A. Williams, and O. Avenel, Phys. Rev. B **34**, 7617(1986).

[38] R.P. Feynmann, R.B. Leighton, and M. Sand, *The Feynmann Lectures on Physics*, Vol. I (Addison-Wesley, Reading, 1963). Ch.31.

[39] R.N. Shakhmuratov, Phys. Rev. A **85**, 023827 (2012).

[40] D.C. Burnham and R.Y. Chiao, Phys.Rev. **188**, 667 (1969).

[41] M.D. Crisp, Phys. Rev A **1**, 1604 (1970).

[42] A. Laubereau and W Kaiser, Rev. Mod. Phys. **50**, 607 (1978).

[43] Yu.M. Kagan, A.M. Afanas'ev and V.G. Kohn, J. Phys. C **12**, 615 (1979).

[44] H.J. Hartmann and A. Laubereau, Opt. Commun. **47**, 117 (1983).

[45] B. Macke, J. Zemmouri, and B. Ségard, Opt. Commun. **59**, 317 (1986).

[46] J. Aaviksoo, J. Lippmaa, and J. Kuhl, J. Opt. Soc. Am. B **5**, 1681 (1988).

[47] The integral of Eq.(33) is sometimes expressed in terms of two series of Bessel functions of ascending order, converging in complementary time domains [28, 41, 46]. As remarked in [39], the convergence of these series may be very slow.

[48] W.R. LeFew, S. Venakides, and D.J. Gauthier, Phys. Rev. A **79**, 063842 (2009).

[49] B. Ségard and B. Macke, Opt. Commun 38, 96 (1981).

[50] H. Jeong, A.M.C. Dawes, and D.J. Gauthier, J. Mod. Opt. **58**, 865 (2011).

[51] D. Frohlich, A. Kulik, B. Uebbing, A. Mysyrowicz, V. Langer, H. Stolz, and W. von der Osten, Phys. Rev. Lett. **67**, 2343 (1991). See Fig.1 in this paper.

[52] O. Avenel, E. Varoquaux, and G.A. Williams, Phys. Rev. Lett. **53**, 2058 (1984).

[53] H. Jeong and U. Österberg, J. Opt. Soc. Am. B **25**, 1 (2008)